

DEVELOPMENT OF EVALUATION METHOD FOR SEISMIC ISOLATION SYSTEMS OF NUCLEAR POWER FACILITIES - BREAK TEST OF FULL SCALE LEAD RUBBER BEARINGS FOR NUCLEAR FACILITIES,

PART3 FINITE ELEMENT ANALYSIS MODEL FOR BREAK TEST-

Takahiro Mori¹, Nobuo Masaki², Nobuo Murota³, Takafumi Hiraki⁴, Masaki Ikeda⁵, Hiroshi Shimizu⁶, Masakazu Jimbo⁷, Takashi Nakayama⁸ and Yoshito Umeki⁹

¹ Infrastructure Products Development Department, Bridgestone Corporation, Japan

² Fellow, Infrastructure Products Development Department, Bridgestone Corporation, Japan

³ General Manager, Infrastructure Products Development Department, Bridgestone Corporation, Japan

⁴ Research Engineer, Central Research Institute of Electric Power Industry (CRIEPI), Japan

⁵ Staff Engineer, Aseismic Engineering Sec., Nuclear Plant Engineering Dept., Hitachi-GE Nuclear Energy, Ltd, Japan

⁶ Structure No.1 Lab., Strength Research Dept., Research & Innovation Center, Mitsubishi Heavy Industries, Ltd., Japan

⁷ Chief Specialist, Plant Design & Engineering Dept., Isogo Nuclear Engineering Center , Toshiba Corporation Power Systems Company, Japan

⁸ Senior Manager, Structural Engineering Nuclear Power Department, Kajima Corporation, Japan

⁹ Manager, Nuclear Power Plant Arch. Eng. Section, Civil & Arch. Dept., Chubu Electric Power Co. Inc., Japan

ABSTRACT

In the previous report, other part of this series of papers (Imaoka et al. (2015) and Nakayama et al. (2015)), break test results of full-scale lead rubber bearing (LRB) were shown. In this report, we propose finite element analysis (FEA) model which can trace the break test results for the purpose of prediction of LRB break characteristics. In the case of modelling FEA for rubber bearings, selection of material model for rubber is important. As a rubber material model, we select hyper-elastic model which can represent the softening under tri-axial tensile deformation.

First, details of proposed FEA model are shown. Second, we show the validity of proposed model by comparing with break test results of relation between shear/tensile stress and shear/tensile strain. Finally, breaking criteria of LRB is suggested.

INTRODUCTION

Now, according to the growing of a computing technology, application of numerical simulation design for structures, products, materials and so on has become general. In this report, we propose finite element analysis (FEA) model which can trace the break test results for the purpose of prediction of LRB break characteristics reported in previous report (Imaoka et al. (2015) and Nakayama et al. (2015)). In the case of modelling lead rubber bearing (LRB), selection of material model for rubber is very important. In the past, various material models for rubber are proposed e.g. Yeoh (1993), Ogden (1998), etc. In order to trace the property of tensile deformation of LRB, material model which can represents the reduction of stiffness under tensile deformation caused by generation of void in rubber is needed. In the past, material model which can represent its reduction stiffness behavior is proposed by Mori et al. (2011). In this report, we show the developed prediction technique using FEA model with proposed rubber material model.

First, details of proposed FEA model are shown. Second, we show the validity of proposed model by comparing with break test results of relation between shear/tensile stress and shear/tensile strain. Finally,

breaking criteria of LRB is suggested to predict break characteristics of LRB and parameter studies are performed for the purpose of improvement of breaking characteristics.

FEA MODELLING OF LRB

In the case of modelling rubber bearings, selection of material model for rubber and its values of material parameters are important. In this section, outlines of the FEA model including material model for rubber and determination result of material parameters are shown.

Outlines of FEA Model

FEA model for determination of rubber material parameters are shown in Figure 1. If nodes are shared at a boundary between lead and rubber/plate, stable analysis results are obtained. Therefore, in the case of calculating horizontal loading under compression, nodes of inner rubber and insert plate are shared with lead, because vertical deformation is small. However, since horizontal deformation is large in the case of vertical tensile loading, node share boundary condition is not valid and contact condition must be used. If contact condition is used at boundary between lead and inner rubber/insert plate, analysis becomes unstable. Therefore, in almost all of the case, modelling of lead plug is omitted because it is assumed that lead does not affect the result of break characteristics. Details of selected element for each material are shown in Table 1, and boundary conditions are shown in Table 2.

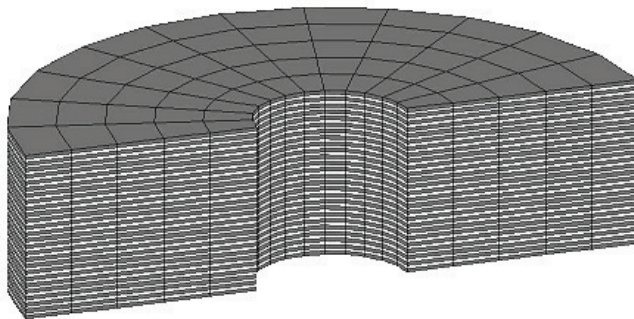


Figure 1. FEA model for determination of rubber material parameters

Table 1. Element types

Material	Element type
Inner rubber	8-nodes hexahedral element (full integral)
Insert plate	8-nodes hexahedral element (reduced integral)
Lead plug (if modelling)	8-nodes hexahedral element (full integral)

Table 2. Boundary conditions

Boundary of each materials	Node share
Lower surface of LRB	Fixed
Upper surface of LRB	Tying with dummy node which has 2 DOF for vertical and horizontal loading direction
Symmetric surface	Fixed for normal direction of symmetric surface

Material Model and Material Parameters

Material model for inner rubber is given by,

$$W = W_{\text{dev}} + W_{\text{vol}} \quad (1)$$

$$W_{\text{dev}} = a(I_1 - 3) + b(I_1 - 3)^3 \quad (2)$$

$$\begin{cases} W_{\text{vol}} = \frac{1}{2} \kappa_1 (J - 1)^2 & (J - 1 \leq 0) \\ W_{\text{vol}} = \frac{1}{2} \kappa_2 (J - 1)^2 & (0 < J - 1 \leq \varepsilon_1) \\ W_{\text{vol}} = \frac{1}{2} \kappa_3 (J - 1)^2 + \varepsilon_1 (\kappa_2 - \kappa_3) (J - 1) - \frac{1}{2} (\kappa_2 - \kappa_3) \varepsilon_1^2 & (\varepsilon_1 < J - 1) \end{cases} \quad (3)$$

where, W is strain energy density function, W_{dev} is deviatoric part of W , W_{vol} is volumetric part of W , I_1 is first invariant of right Cauchy-Green tensor and J is invariant representing volume change. This model can represents the reduction of stiffness under tensile deformation caused by generation of void in rubber. a , b , κ_1 , κ_2 , κ_3 and ε_1 are material parameters. a represents linear spring constant, b represents magnitude of hardening behavior at the range of large shear strain, κ_1 represents the compressive modulus, κ_2 represents tensile modulus, κ_3 represents tensile modulus after yielding and ε_1 represents the yielding tensile strain. a and b are determined to make shear stress – shear strain relationship of analysis result correspond with that of test result of horizontal loading under compressive stress 0MPa. In the case of determining a and b , material model represented by Equation (4) is used for inner rubber for simplicity.

$$W = a(I_1 - 3) + b(I_1 - 3)^3 + \frac{9}{2} \kappa_1 (J^{1/3} - 1)^2 \quad (4)$$

κ_2 , κ_3 and ε_1 are determined to make tensile stress – tensile strain relationship of analysis result correspond with that of test result of vertical tensile loading under offset=0%. Since it is difficult to determine κ_1 , κ_1 is set to 1000MPa. Details of analysis conditions are shown in Table 3.

Material model for insert plate and lead plug are bi-linear plastic-elastic model whose yielding condition is Mises condition, and material parameter values are shown in Table 4.

Table 3. Analysis conditions

Load case	Analysis condition	Comparison target of test results	Identified parameters
Horizontal shear loading	Monotonic horizontal loading up to shear strain 450% by displacement control under 0MPa of compressive pressure.	Test result of relation between shear stress and shear strain performed in 2013.	a, b
Vertical tensile loading	Vertical tensile loading up to 4MPa by load control under 0% of offset shear strain.	Test result of relation between tensile stress and tensile strain performed in 2013.	$\kappa_2, \kappa_3, \varepsilon_1$

Table 4. Material parameters for insert plate and lead plug

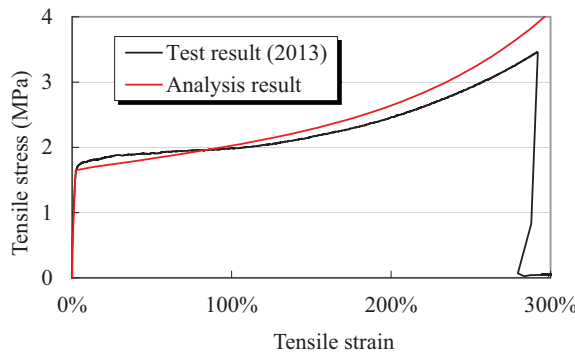
	Young modulus (MPa)	Poisson ratio (-)	Yield stress (MPa)	Modulus after yielding (MPa)
Insert plate	205000	0.3	235	2050
Lead plug	270	0.3	12	2.7

Determination Result of Material Parameters of Rubber

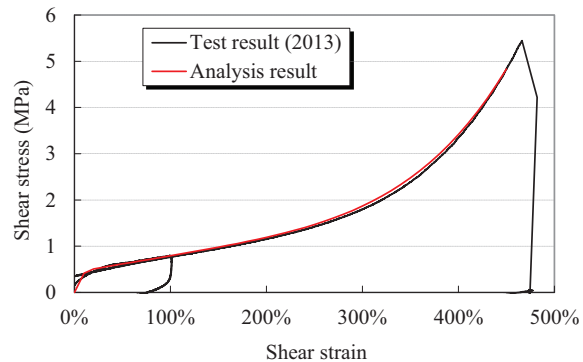
Identification result of material parameters are shown in Table 5, and comparison with test results are shown in Figure 2. As can be seen from Figure 2, analysis result shows good agreement with test result.

Table 5. Identification result of material parameters of rubber

a (MPa)	b (MPa)	κ_1 (MPa)	κ_2 (MPa)	κ_3 (MPa)	ε_1 (-)
0.175	0.00026	1000	60	0	0.022



(a) Vertical tensile loading



(b) Horizontal loading (lead plug are modeled limited only this case)

Figure 2. Comparison with test results in 2013
 (See Table. 3 for comparison target of test result)

Validation of FEA Model by Comparing Test Results

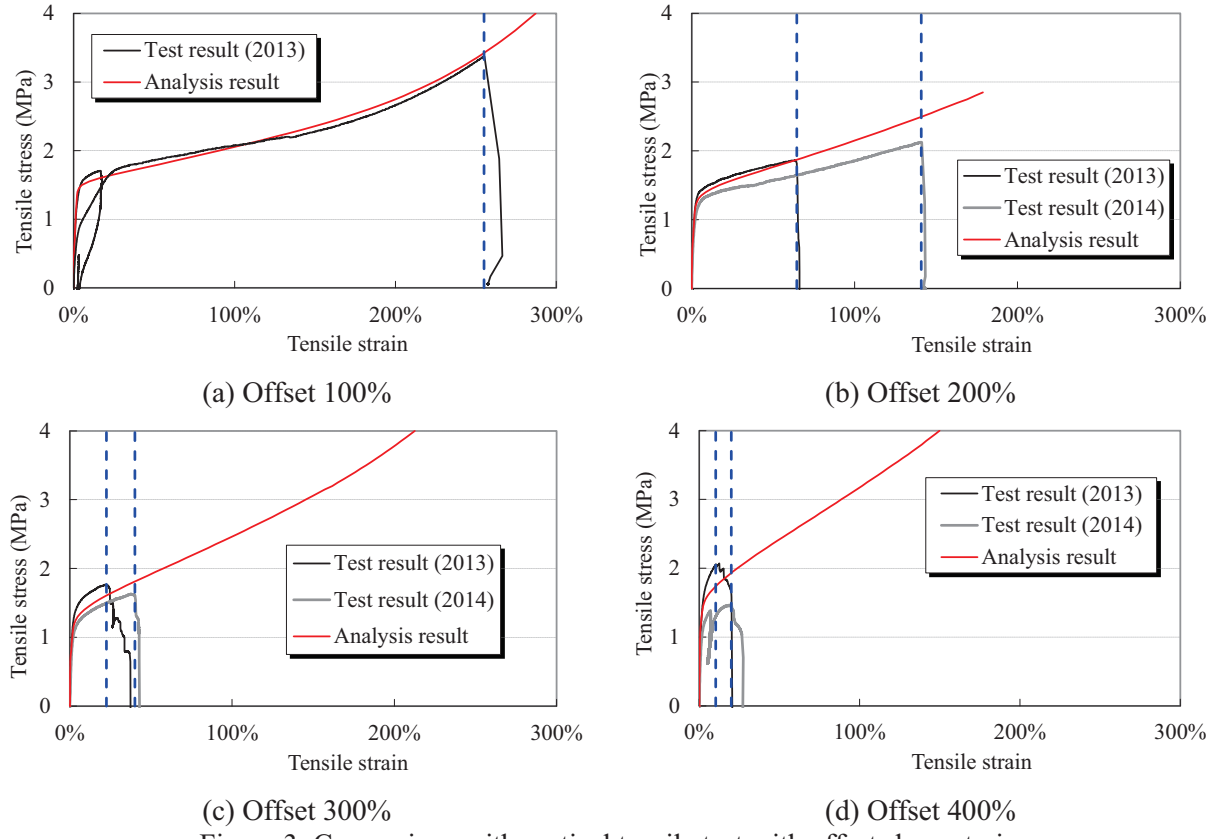
Preceding definition of break criteria, comparison with vertical tensile test under each offset strain is shown to examine the validity of proposed FEA model. Analysis conditions are shown in Table 6, and comparison results are shown in Figure 3. As can be seen from Figure 3, analysis result can well simulate the vertical tensile behaviour.

Table 6. Analysis conditions

Vertical tensile loading	Offset shear strain
Vertical tensile loading up to 4MPa by load control.	100%
	200%
	300%
	400%

DEVELOPMENT OF PREDICTION TECHNIQUE OF BREAK CHARACTERISTICS FOR LRB

If predicting break characteristics, break criteria of target material must be clarified. In this section, breaking criteria of LRB is suggested to predict break characteristics of LRB and parameter studies are performed to improve performance of the tensile ultimate characteristics.



Defining Method of Break Criteria for LRB

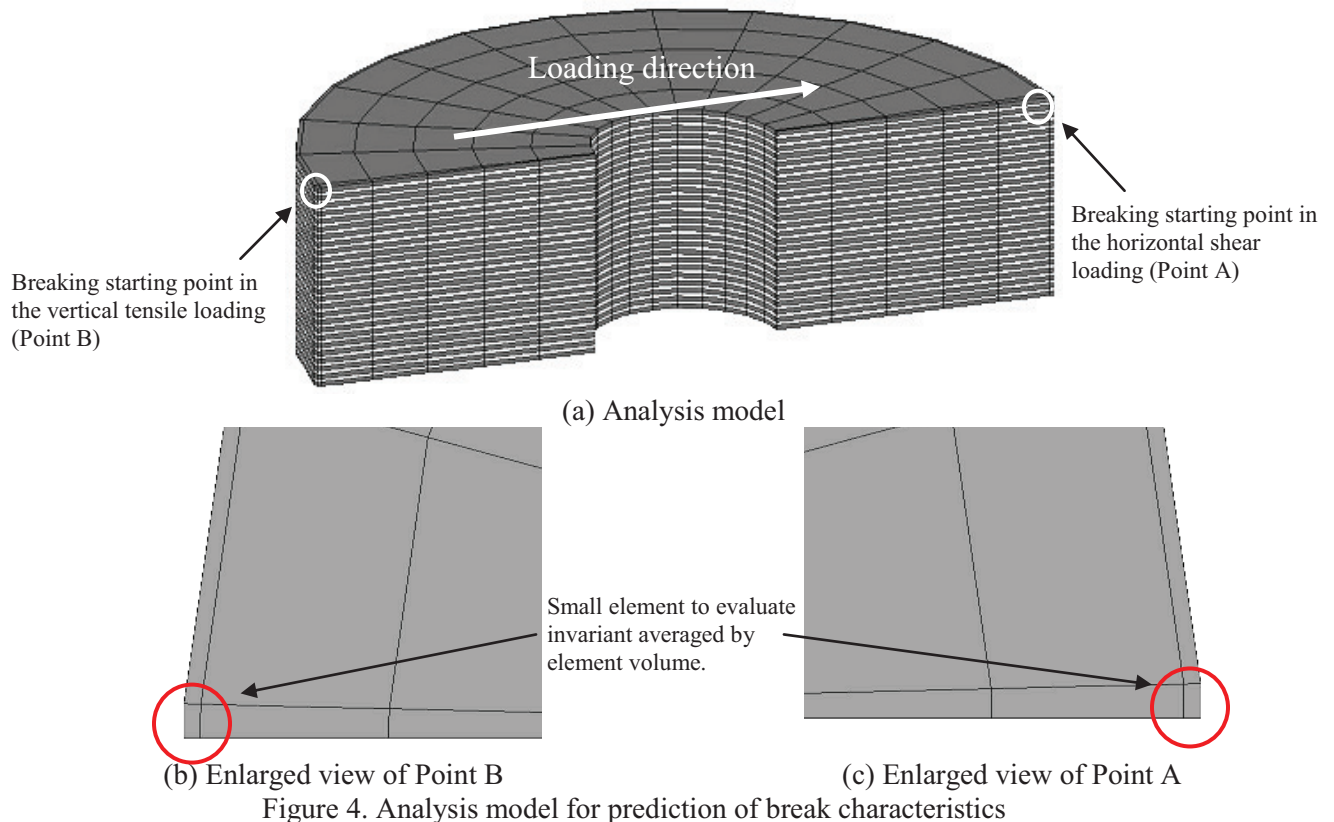
First, defining method of break criteria for LRB is shown. Break criteria is defined by examining the state of strain of breaking point at the moment LRB breaks. Break criteria is defined as a function of principal stretch ratio λ_1 , λ_2 and λ_3 . λ_1 , λ_2 and λ_3 are maximum, medium, minimum principal stretch ratio respectively. Meshes examined principal stretch ratio are shown in Figure 4, and analysis conditions are shown in Table 7 and 8.

Table 7. Analysis conditions of horizontal shear loading

Analysis No.	Compressive stress	Horizontal shear loading condition
H-m1	-1MPa (Tensile stress)	Monotonic loading up to shear strain 500%.
H-00	0MPa	
H-05	5MPa	
H-08	8MPa	

Table 8. Analysis conditions of vertical tensile loading

Analysis No.	Vertical tensile loading condition	Offset strain
V-00	Monotonic tensile loading	0%
V-01	Monotonic tensile loading after loading offset shear strain under compressive stress 0MPa.	100%
V-02		200%
V-03		300%
V-04		400%



Analysis Results

Contour figures of Green-Lagrange strain at the moment when LRB breaks at the vertical tensile test are shown in Figure 5. As can be seen from Figure 5, the point which tends to become breaking start (Point B) shows maximum value in analysis result. In the case of offset=200%, strain value has widely distributed compared with other offset case. Therefore, local vertical strain at breaking point is largely different from total vertical strain of LRB. This is why, tensile breaking strain at offset=200% is largely reduced from that at offset=100%.

Definition of Breaking Criteria

Analytically obtained values of principal stretch ratios λ_1 , λ_2 and λ_3 at breaking point at the moment LRB breaks in the test are shown in Table 9. γ and ε denote shear and tensile strain respectively. As can be seen from Table 9, λ_2 indicate almost 1 independent of loading condition, so it can be regarded that breaking point is plane-strain state. Maximum principal stretch ratios λ_1 , on the other hand, indicate approximately 4 independent of loading condition. According to this result, it is assumed that breaking of LRB occurs when λ_1 reaches certain threshold value at breaking point. Therefore, breaking criteria is defined as $\lambda_1=B_{cr}$. There is a possibility which predict breaking strain of LRB by calculating shear/tensile strain at the moment when λ_1 reaches certain threshold value B_{cr} at breaking point A or B.

As a result of calculating B_{cr} by least-square method, threshold value is obtained as $B_{cr}=4.36$. A figure plotted B_{cr} values at breaking point at the moment LRB breaks is shown in Figure 6 in each analysis. Blue solid line denotes threshold value $B_{cr}=4.36$. Whereas variability inevitably exists, when λ_1 reaches 4.36 in analysis, break occurs in break test. A comparison between test results of break test and breaking curve predicted by FEA is shown in Figure 7.

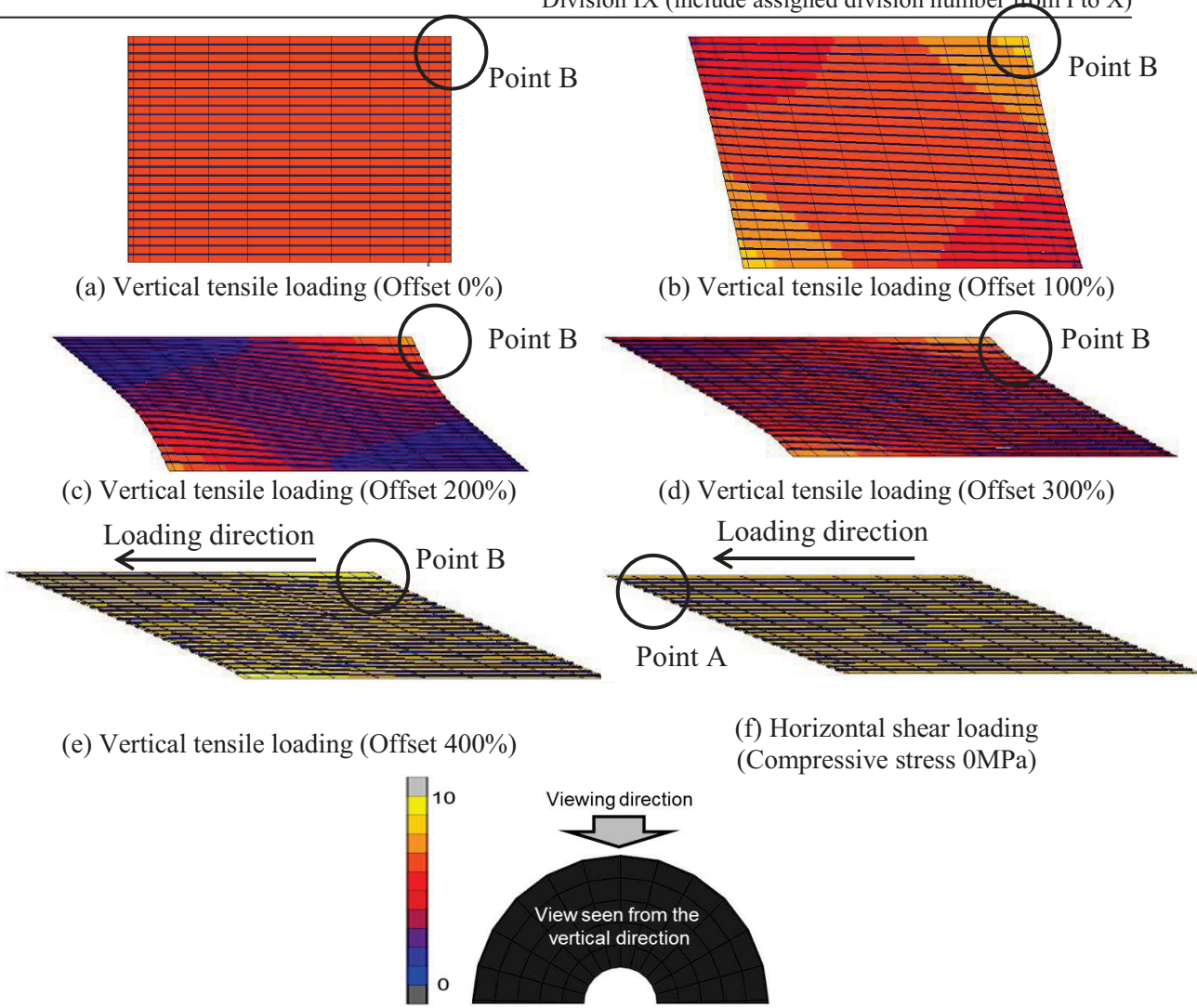


Figure 5. Maximum principal strain contours at the moment of break generated in test

Table 9. Analytical value of each invariant at the moment of break generated in test

Analysis No. *1 (Breaking start point)	Compressive stress	Offset strain	Analytical value of each invariant				Breaking shear/tensile strain
			λ_1	λ_2	λ_3	J	
H-m1 (Point A)	-1MPa	-	4.14	1.00	0.24	1.01	$\gamma=3.94$
H-00 (Point A)	0MPa	-	4.90	1.00	0.21	1.01	$\gamma=4.66$
H-05 (Point A)	5MPa	-	4.70	1.00	0.22	1.01	$\gamma=4.48$
H-08 (Point A)	8MPa	-	4.69	1.00	0.22	1.01	$\gamma=4.47$
V-00 (Point B)	-	0%	3.91	1.00	1.00	3.91	$\varepsilon=2.91$
V-01 (Point B)	-	100%	4.23	1.00	0.97	4.11	$\varepsilon=2.55$
V-02a (Point B)	-	200%	3.90	1.00	0.86	3.36	$\varepsilon=0.63$
V-03a (Point B)	-	300%	4.04	1.00	0.64	2.57	$\varepsilon=0.22$
V-04a (Point B)	-	400%	4.53	1.00	0.41	1.85	$\varepsilon=0.11$
V-02b (Point B)	-	200%	4.34	1.00	0.89	3.88	$\varepsilon=1.41$
V-03b (Point B)	-	300%	4.26	1.00	0.69	2.94	$\varepsilon=0.37$
V-04b (Point B)	-	400%	4.67	1.00	0.46	2.16	$\varepsilon=0.18$

*1 V-02a – V-04a denotes test results in 2013 and V-02b – V-04b denotes test results in 2014.

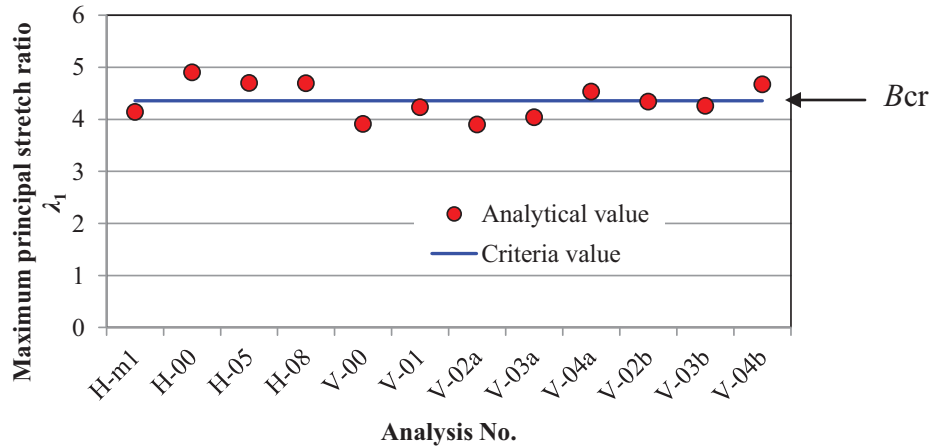


Figure 6. Comparison between criteria B_{cr} and λ_1 at the moment of break generated in test

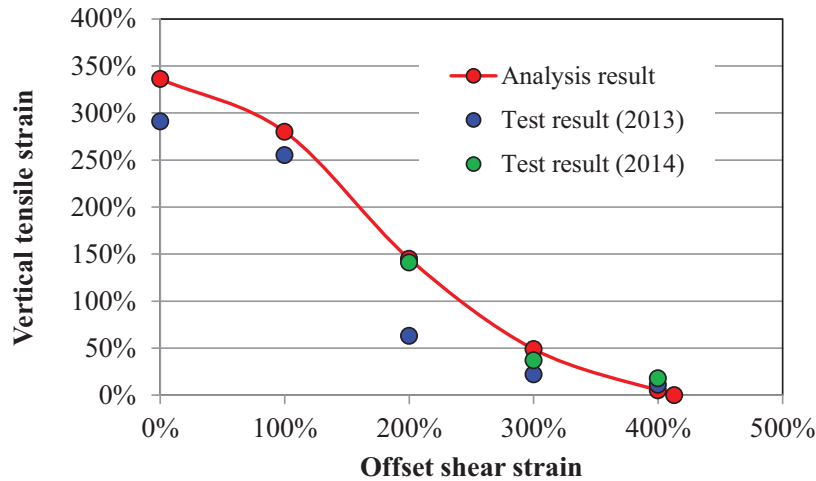


Figure 7. Comparison between break test result and break curve obtained from FEA analysis

PARAMETER STUDY BASED ON PROPOSED BREAKING CRITERIA

In this section, by performing parameter study which changes thickness of inner plate or rubber, we perform feasibility study whether change of such structure improved breaking characteristics. In this report, we perform 2 cases of analysis in addition to current structure. One is the case where number of rubber layer doubles and thickness of rubber halves (Structure B). The other is the case where thickness of insert plate doubles (Structure C). (Current structure is ‘Structure A’) By comparing breaking curve obtained in previous section with that of parameter study analysis, we examined whether there are effects of improvement of breaking characteristics. Dimension of LRB calculated in parameter study is shown in Table 10.

Contour figures of maximum principal strain of Green-Lagrange strain at the moment when LRB breaks at the vertical tensile test are shown in Figure 8. As can be seen from Figure 6, Structure B and C shows low value of Green-Lagrange strain at breaking point compared with current structure A.

Calculation result of breaking curve is shown in Figure 9. As can be seen from Figure 9, effect of improvement of breaking characteristics is confirmed.

Table 10. Dimension of rubber bearing of analysis model for parameter study

	Structure A (Current structure)	Structure B (Double layers)	Structure C (Double thickness of insert plate)
Rubber thickness (mm)	10	5	10
Number of layer	26	52	26
Total rubber thickness (mm)	260	260	260
Diameter of lead (mm)	392	392	392
Thickness of insert plate (mm)	6.8	6.8	13.6

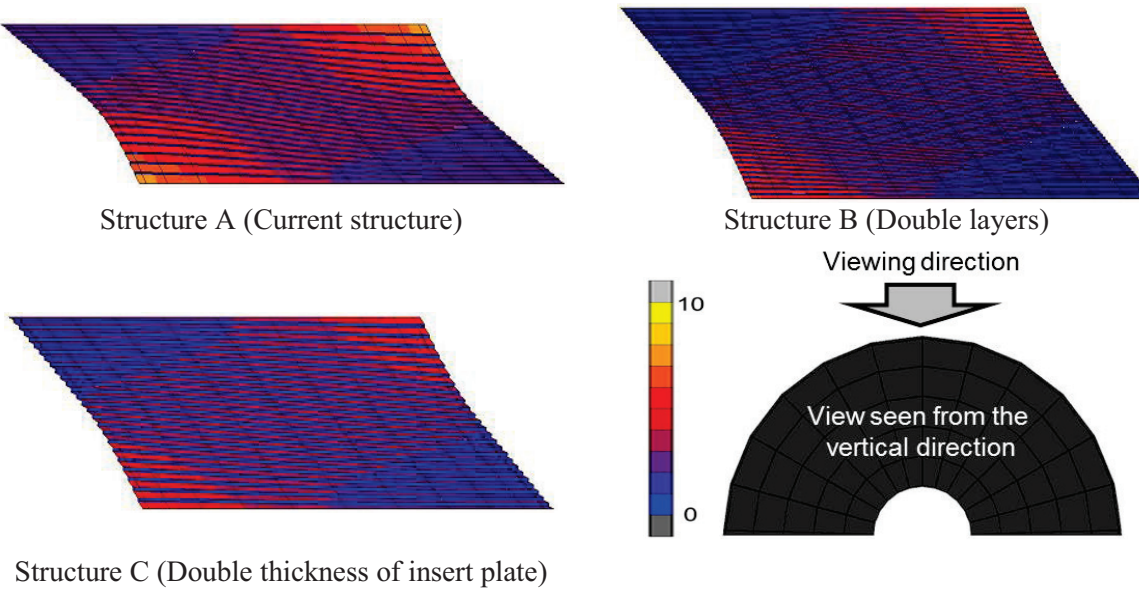


Figure 8. Maximum principal strain contours at the moment of break generated in test

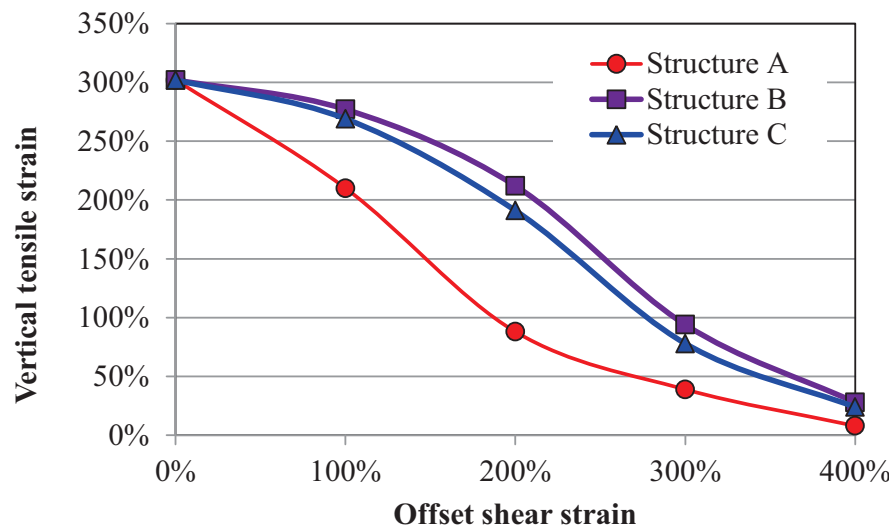


Figure 9. Break curve predicted by FEA analysis

CONCLUSION

We developed an FEA model which can predict the ultimate state of LRB by determining the break criteria of rubber and examined the validity of the model by comparing LRB break test. Important summary of analysis condition of proposed FEA model is shown as follows;

- FEA model : 3-Dimensional (Modelling of materials are inner rubber and insert plate only).
- Material model for rubber : Material model which can represents the reduction of stiffness under tensile deformation caused by generation of void in rubber.
- Breaking criteria of rubber : Maximum principal stretch ratio.

By applying developed prediction technique, it may be possible to design LRB considering ultimate characteristics. However, application range of developed prediction technique is not clear. Therefore, it is remaining issue of this study to examine accuracy of the FEA model by comparing other cases of break test result.

ACKNOWLEDGMENTS

This technology development has been carried out as Japan national project “Development of Evaluation Method for Seismic Isolation Systems of Nuclear Power Facilities” with the participation of Chubu Electric Power, Japan Atomic Power, Hokkaido Electric Power, Tohoku Electric Power, Tokyo Electric Power, Hokuriku Electric Power, Kansai Electric Power, Chugoku Electric Power, Shikoku Electric Power, Kyushu Electric Power, J Power, Toshiba, Hitachi-GE Nuclear Energy, Mitsubishi Heavy Industries, and the Institute of Applied Energy.

We thank Dr. Nishikawa, a Professor Emeritus at Tokyo Metropolitan University, Dr. Kubo, a Professor Emeritus at the University of Tokyo, Dr. Fujita, a Professor Emeritus at the University of Tokyo, Dr. Kasahara, a Professor at the University of Tokyo, Dr. Yabana, the Central Research Institute of Electric Power Industry for their advice.

REFERENCES

- Imaoka, T. et al.(2015), “Development of Evaluation Method for Seismic Isolation Systems of Nuclear Power Facilities, -Break Test of Full Scale Lead Rubber Bearings for Nuclear Facilities, Part 1,” Trans of the twenty-third Structural Mechanics in Reactor Technology (SMiRT-23), Manchester, UK .
- Nakayama, T. et al.(2015), “Development of Evaluation Method for Seismic Isolation Systems of Nuclear Power Facilities, -Break Test of Full Scale Lead Rubber Bearings for Nuclear Facilities, Part 2,” Trans of the twenty-third Structural Mechanics in Reactor Technology (SMiRT-23), Manchester, UK .
- Ogden, R. W., (1998) “Nonlinear Elastic Deformations”, Dover.
- Yeoh, O. H., (1993) “Some forms of the strain energy function for rubber”, *Rubber Chemistry and technology*, Volume 66, Issue 5, 754-771.
- Mori, T., Kato, H., Kikuchi, T., and Murota, N., (2011). “Elastic-plastic constitutive law of rubber for laminated rubber bearings.”, *12th World Conference on Seismic Isolation Energy Dissipation and Active Vibration Control of Structures*.